



저작자표시-비영리-변경금지 2.0 대한민국

이용자는 아래의 조건을 따르는 경우에 한하여 자유롭게

- 이 저작물을 복제, 배포, 전송, 전시, 공연 및 방송할 수 있습니다.

다음과 같은 조건을 따라야 합니다:



저작자표시. 귀하는 원저작자를 표시하여야 합니다.



비영리. 귀하는 이 저작물을 영리 목적으로 이용할 수 없습니다.



변경금지. 귀하는 이 저작물을 개작, 변형 또는 가공할 수 없습니다.

- 귀하는, 이 저작물의 재이용이나 배포의 경우, 이 저작물에 적용된 이용허락조건을 명확하게 나타내어야 합니다.
- 저작권자로부터 별도의 허가를 받으면 이러한 조건들은 적용되지 않습니다.

저작권법에 따른 이용자의 권리는 위의 내용에 의하여 영향을 받지 않습니다.

이것은 [이용허락규약\(Legal Code\)](#)을 이해하기 쉽게 요약한 것입니다.

[Disclaimer](#)

공학석사 학위논문

**A Study on the process parameter dependent  
electrical conductivity of Poly Vinyl Alcohol (PVA)-  
Carbon Nanotube (CNT) composite films**

폴리비닐알콜과 탄소나노튜브 복합체 필름의 공정 변수에  
따른 전도 특성에 관한 연구

2015년 2월

서울대학교 대학원

융합과학부 나노융합전공

이 중 환

**A Study on the process parameter dependent  
electrical conductivity of Poly Vinyl Alcohol (PVA)-  
Carbon Nanotube (CNT) composite films**

폴리비닐알콜과 탄소나노튜브 복합체 필름의 공정변수에 따른  
전도 특성에 관한 연구

지도교수 송 윤 규

이 논문을 공학석사 학위논문으로 제출함

2015년 1월

서울대학교 대학원  
융합과학부 나노융합전공

이 종 환

이종환의 석사 학위논문을 인준함

2015년 1월

위 원 장 박 원 철 (인)

부위원장 송 윤 규 (인)

위 원 Jan Lagerwall (인)

# **Abstract**

## **A Study on the process parameter dependent electrical conductivity of Poly Vinyl Alcohol (PVA)– Carbon Nanotube (CNT) composite films**

JongHwan Lee

Program in Nano science and Technology

The Graduate School

Seoul National University

Carbon Nanotubes (CNT) have long been considered an attractive material for applications, due to their outstanding electric properties. However, this kind of Carbon material has dispersion problems when used as filler in composites with other polymers.

In particular, one of the main obstacles in Carbon nanotube applications is large aggregation, caused by the van der Waals force among the carbon nanotubes. Van der Waals attraction occurs when a fluctuation-induced dipole in one CNT induces an opposing dipole in an adjacent CNT. In this situation, each CNT particle can easily attract other particles via van der Waals force, which causes large aggregations in CNTs. For these reasons, it is challenging to get CNT materials to disperse into a solvent. This can result in an increased amount of CNT required for percolation . It also means that materials might be wasted in making a path for conducting electricity. In other words, it requires

excessive CNT to reach its percolation threshold.

Particularly in the case of polymer composites with CNT particles, aggregated particles play a role in deteriorating the electrical properties. Therefore, in this research, we have tried to make a well-dispersed CNT suspension with a surfactant and made a composite film with a PVA polymer.

First, to find the optimum condition for the dispersion of CNT, CNT particles were mixed with a surfactant in a distilled water solvent. CTAB, which is a cationic surfactant, was used as a surfactant. After that, we also investigated the optimum sonication time conditions for CNT dispersion.

Through this step, we can conclude the optimal sonication time for the best dispersion, avoiding damaging the CNT. Furthermore, we make certain that long sonication can damage CNT morphology via Raman spectroscopy. For this reason, we tried to avoid damage as much as possible, and to select the well dispersed CNT, we introduced a centrifugation step after dispersion and making the supernatant for the composite with PVA. In addition, we have examined the surfactant concentration for an effective dispersion state, and we have calculated the CNT loss amount after centrifuging via optical absorbance.

After optimizing all conditions, we made a film via the drop-casting method and checked electrical conductivities. The conductivity was approximately  $4 \cdot 10^{-6}$  S/cm at PVA–CNT mass ratio 10:1, and began to increase rapidly as the PVA–CNT mass ratio increased to 8:1, and finally reached approximately 2 S/cm at a PVA–CNT mass ratio of 1:10.

**Keywords(5) : Carbon nanotubes (CNTs), Polymer Composite, Poly vinyl alcohol(PVA), films,**

**Conductivity**

**Student Number : 2012-22450**

# Contents

<b>Abstract</b> .....	I
<b>Contents</b> .....	III
<b>List of table and figures</b> .....	V

## 1. Motivation and Goals

## 2. Introduction

2.1 Single-Wall Carbon Nanotube

2.2 Poly vinyl alcohol

2.3 Percolation threshold

2.4 Van der Pauw method

2.5 Raman spectroscopy

## 3. Experimental Process

3.1 Materials and characterization

3.2 Process of CNT dispersion

3.3 PVA–CNT composite and fabrication film

3.4 Electric properties PVA–CNT composite film

3.5 Mechanical properties of PVA–CNT composite film

## **4. Result and Discussion**

4.1 Assessment of CNT dispersion quality

4.2 Optical characterization of PVA–CNT composite films prepared following different protocols

4.4 The electrical properties of PVA–CNT composite film

4.5 The mechanical properties of PVA–CNT composite film

## **5. Conclusion**

## **References**

요 약 (국문초록)

# List of Figures and Table

**Figure 1.** A flat graphene sheet and the rolling orientation for different types of SWCNT.

**Scheme 1.** Simple mechanism of the synthesizing step of PVA. (A) Synthesizing vinyl acetate precursor. (B) Synthesizing polyvinyl alcohol via the saponification of PVAc.

**Figure 2.** Simplification of percolation model in two dimensions. (A) Particles exist independently in the matrix. ( $P < P_c$ ) (B) Particles make a network in the matrix. ( $P > P_c$ )

**Figure 3.** A simple mimetic diagram to illustrate the van der Pauw method. The left setup is for getting the sheet resistance measured by the vertical axis ( $R_A$ ), and the right setup is measured by the vertical axis ( $R_B$ ).

**Scheme 2.** The simple set-up scheme of Raman spectroscopy.

**Figure 4.** Electrode set up for measuring the electric conductivity via the van der Pauw method.

**Table 1.** List of conditions for CNT concentration and kind of surfactant and surfactant concentration.

**Figure 5.** CNT dispersion state for the corresponding surfactant condition and sonication time dependence. (The scale bar corresponds to 50  $\mu\text{m}$ )

**Figure 6.** 1 mg/ml CNT with 10 mg/ml CTAB surfactant suspension distribution of particle size, following the sonication time dependence by DLS. (A) 30 min sonication (B) 60 min sonication (C) 90 min sonication (D) 120 min sonication (E) particle distribution of only 10 mg/ml CTAB with water

solvent.

**Figure 7.** Raman D bands ( $1327\text{ cm}^{-1}$ ) and G bands ( $1575\text{ cm}^{-1}$ ) of SWCNT following different sonication time. The more sonication time lead to increase D peak intensity. D peak intensity increase following orders (pristine SWCNTs (black line) < 40 min sonicated SWCNT (blue line) < 180 min sonicated SWCNT (red line))

**Figure 8.** Optical spectra series of dispersed CNT suspension from different CTAB surfactant amount 2 mg/ml to 10 mg/ml.

**Figure 9.** Optical spectra series of dispersed CNT suspension from different kinds of surfactant. (A) 0.2–1.0 mg/ml CNT concentration dispersion with 2 mg/ml CTAB (B) 0.2–1.0 mg/ml CNT concentration dispersion with 2 mg/ml SDBS

**Figure 10.** Supernatant of SWCNT 1 mg/ml with CTAB surfactant 10 mg

**Figure 11.** Visible light absorbance of the CNT suspension following concentration dependence in at 650 nm wavelength. (C) 1 mg/ml CNT suspension with 1 wt% CTAB surfactant.

**Figure 12.** Optical microscope image of the dried PVA–CNT composite solution following sonication time dependence after mixing. (A) 0 min sonication (just 5 min stirring) (b) 30 min sonication (c) 1 hour sonication (d) 1.5 hour sonication (e) 2 hour sonication.

**Figure 13.** SEM images of the PVA–CNT composite film morphology. (A) Whole image of PVA–

CNT 1:10 mass ratio film. (B) Enlarged CNT branch part. (C) Enlarged B image. (D) Whole image of the PVA–CNT 1:5 mass ratio film. (E) Enlarged CNT branch of PVA–CNT 1:5 mass ratio. (F) Enlarged E image.

**Figure 14.** SEM image of the PVA–CNT composite film morphology. (A) Image of PVA–CNT 1:1 mass ratio film. (B) Image A enlarged. (C) Image of PVA–CNT 5:1 mass ratio film. (D) Image B enlarged. (E) Image of PVA–CNT 10:1 mass ratio film. (F) Image E enlarged.

**Table 2.** Conditions for making the PVA–CNT composite solution.

**Figure 15.** I–V curves when applying current each axis measured by van der Pauw method. (A) I–V curves of PVA–CNT 1:5 mass ratio. (B) I–V curves of PVA–CNT 1:1 mass ratio. (C) I–V curves of PVA–CNT 5:1 mass ratio

**Table 3.** Sheet resistance of PVA–CNT composite film with different axis current applying.

**Table 4.** Bulk resistivity and conductivity of the PVA–CNT composite film

**Figure 16.** Conductivity of the PVA–CNT composite films. “0” means only PVA material, and “1” means only CNT material in the x-axis.

# 1. Motivation and Goals

CNT materials have garnered much interest, due to the potential uses of their outstanding electric properties.<sup>[1]</sup> It is well known that single wall CNT (SWCNT) may be either metallically conductive or semiconductive<sup>[1]</sup>. Due to this property, there is active research about the fabrication of devices with conducting properties of the CNT as a base. In particular, in the case of SWCNT, there is research for applications in transparent and flexible devices<sup>[3]</sup>, anodes for lithium ion batteries<sup>[4]</sup>, and the automotive sector<sup>[2]</sup>. However, before developing applications for CNT materials, we should solve their dispersion problem. This is critical for taking advantage of the high surface area of nanofillers<sup>[5]</sup>. In addition, this aggregation causes a key problem by downgrading the performance of the CNT application and wasting material.

PVA is a polymer that can make flexible, transparent fiber very easily and has water soluble conditions, despite its insulating properties<sup>[6]</sup>. Consequently, we have tried to use PVA and CNT for a composite that conducts electricity. In this research, we have tried to mix a PVA solution with a suspension of well dispersed CNTs, evaporate the water to make a dry film, and measuring electric conductivity of these composite films.

PVA–CNT composite can also be applied in the electrospinning process<sup>[7]</sup>. At this time, another of our interests is applying for the electrospinning process with a CNT–polymer composite. The electrospinning process is used to make flexible or reinforced fiber, using various materials such as polymers and ceramics, and it can also be applied for fabricating devices, automobiles, and

sensors<sup>[8],[9]</sup>.

However, in such electrospinning experiments CNT aggregation can cause critical problems. Furthermore, preceding research related to the electric conductivity of PVA–CNT composites should be conducted to satisfy our expectation about electrical conductivity, regardless of making well-made fiber. Therefore, we decide to do preceding research of fabricating PVA–CNT composite films and research detecting its electrical conductivity.

## 2. Introduction

### 2.1 Carbon Nanotubes (CNT)

At the end of the 20<sup>th</sup> century, the nanotechnology field became an attractive avenue for research, and nanotechnology is closely connected to IT, biotechnology, material science, medical science, devices, and energy storage research fields<sup>[10-12]</sup>. This creates vigorous nanomaterials research for each of these sectors. In addition, nano composite materials show possible applications in research areas. In particular, carbon nanotubes (CNT) have garnered interest, due to the potential of using composites as conductive materials.

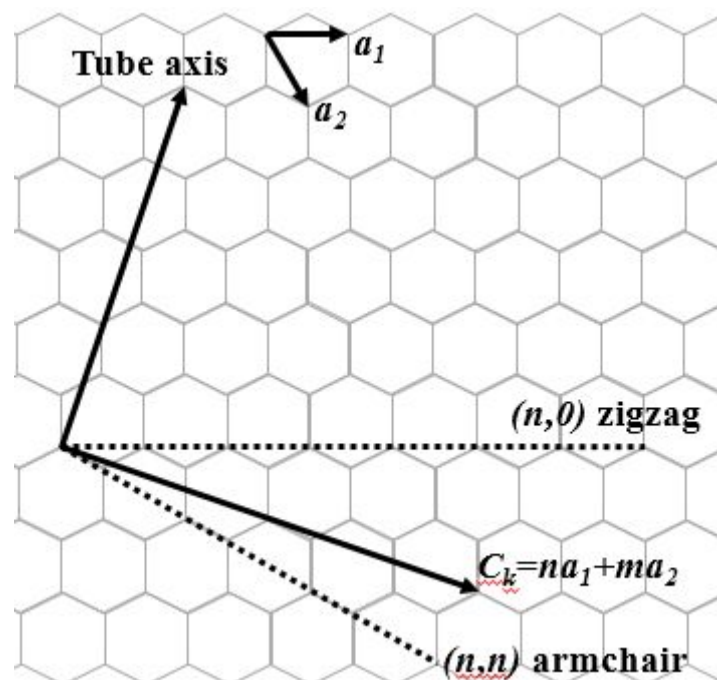


**Figure 1.** A flat graphene sheet and the rolling orientation for different types of SWCNT.

CNT materials can be imagined created by wrapping a graphene sheet on the nanoscale into a tube shape with a diameter of few tens of nanometers, see Fig. 1. In addition, CNT materials have different electrical properties depending on the wrapping direction<sup>[13],[14]</sup>. Normally, 30° wrapped Graphene sheets are called armchair form tube, and they have metallic properties. In addition, 0° wrapped graphene sheet is called a zigzag form tube, and they have semiconducting properties. Moreover, a wrapped Carbon nanotube can have one or more walls. A carbon nanotube with only one wall is called a single wall CNT (SWCNT), and carbon nanotubes with more than one wall are called multi-wall CNT (MWCNT).

SWCNT and MWCNT have very different properties ; as reported in the literature, their Young's moduli are ~1.25 TPa (SWNT) and 0.27–0.95 TPa (MWNT); they have ~200 kS/cm electrical conductivity, ~6600 W/mK (SWNT) and 3000 W/mK (MWNT) thermal conductivity, etc. <sup>[15]</sup>. Carbon Nanotubes (CNT) were reported by Iijima in 1991 and after that, many researchers have studied them actively<sup>[16],[17]</sup>. Nevertheless, to access these interesting potential properties in composites with CNTs, we must retain a CNT dispersion technique with a polymer matrix.

Nowadays, some process methods have been reported for making carbon nanotubes and polymer composites, which are *in situ* polymerization, solution mixing, and melt mixing<sup>[18]</sup>.

Polymer–CNT composites that are made via these process methods can be applied in secondary batteries<sup>[19]</sup>, supercapacitors<sup>[20]</sup>, sensors<sup>[21]</sup>, high strength compound materials<sup>[22]</sup>, etc. Furthermore, they have great potential for performance improvements, depending on the composition of the material<sup>[18]</sup>.

Particularly in the case of CNT materials, many researchers have reported that they can be used to increase the established electric properties of polymers by polymer–CNT composite.

In this research, we have focused using PVA, which is an insulating polymer, and CNT to make composites. After that, we made a film using this composite. Accordingly, this PVA–CNT film had detectable electric conductivity, due to the percolation of the CNT particles.



Although PVA is a high-crystalline polymer, the melting process cannot be used, since it melts and pyrolyzes at a similar temperature<sup>[25]</sup>. Thus, drop casting with aqueous solution is normally used to make a PVA film that is attractive for use as a packaging film, and water soluble film<sup>[25]</sup>.

## 2.3 Percolation theory

A percolation model considers a collection of points distributed in space, certain pairs of which are said to be adjacent or linked<sup>[26]</sup>. These points were called a cluster, or sometimes a monomer in a system. A cluster has fixed independent positions in a system, and sometimes makes random linkages with other clusters.

When we make these linkage paths successfully through an entire system, a transition that affects the macroscopic sample properties occurs. This transition occurs at a definite critical probability  $P_c$ <sup>[27]</sup>, which can be called the percolation threshold.

Following the cluster amount increasing in a matrix, the average linkage probability ( $P$ ) increases. With increasing linkage probability the cluster size increases. When clusters have a lower linkage probability ( $P$ ) than the percolation threshold ( $P_c$ ), they occupy an independent position in the whole system. However, if the linkage probability ( $P$ ) gets higher than the percolation threshold ( $P_c$ ), clusters make conducting path throughout the whole system. Figure 2 shows a simplified version of these phenomena.

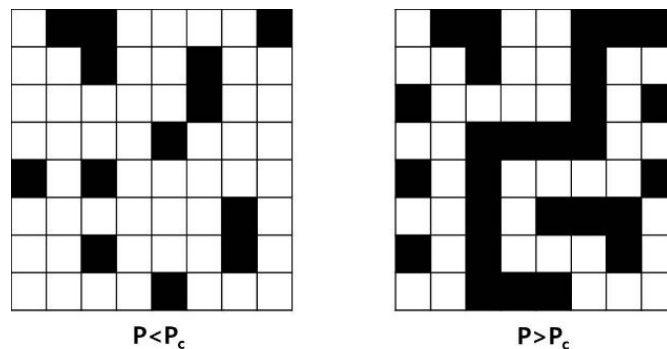


**Figure 2.** Simplification of percolation model in two dimensions. (A) Particles exist independently in

the matrix. ( $P < P_c$ ) (B) Particles make a network in the matrix. ( $P > P_c$ )

In the case of CNT material, there are advantages to connecting itself via a percolation system. Since CNT is tubular and is longer than other material, it can be used to make an easy percolation model with fewer particles than other typical materials.

Therefore, PVA–CNT film, which makes a percolation system this way, percolates CNT in a PVA matrix, and can form a path that can allow electrical conductivity in a matrix. However, in order to prevent aggregation, CNT are in our research coated with the surfactant (CTAB), so hindering the CNT from contacting other adjacent CNT. This means it requires more CNT material than expected.

Accordingly, in this research, we tried to check the degree of percolation through dependence between the electrical conductivity and CNT amount. We determined the percolation threshold by measuring the CNT concentration at which the electric conductivity was drastically increased.

## 2.4 Van der Pauw method

The van der Pauw method is commonly used to measure carrier mobility and carrier concentration. However, when we calculate carrier concentration we must measure the resistivity of the samples<sup>[28]</sup>. Thus, the Van der Pauw method is powerful for measuring resistivity. Additionally, when we measure resistivity using the Van der Pauw technique, we should consider ohmic contact, accurately measuring the thickness, etc.<sup>[29]</sup>

For measuring bulk resistivity, we need to measure the whole sheet resistance ( $R_S$ ). Accordingly, to use the van der Pauw method, we need two characteristic sheet resistances, which are the sheet resistance measured by vertical axis ( $R_A$ ), and measured by the horizontal axis ( $R_B$ ). To measure the sheet resistance along these perpendicular axes, we must first apply a constant current  $I_{12}$ , via ohmic contacts to the surface part (number 1, 2 spot) and then measure the voltage  $V_{43}$  via ohmic contacts to the surface part (number 3, 4 spot). Following this step, we can calculate the sheet resistivity measured by the vertical axis ( $R_A$ ) with  $I_{12}$  and  $V_{43}$ , as shown in Figure 3.

In the same way, we are applying a constant current  $I_{23}$  via ohmic contacts to the surface part (number 2, 3), then measuring the voltage  $V_{14}$  via ohmic contacts to the surface part (number 1, 4). in addition, we can calculate the sheet resistance measured at the horizontal axis ( $R_B$ ) with  $I_{23}$  and  $V_{14}$ . Consequently, the vertical and horizontal sheet resistances are

$$R_A = V_{43} / I_{12} \text{ , } R_B = V_{14} / I_{23} \text{ .....(1)}$$

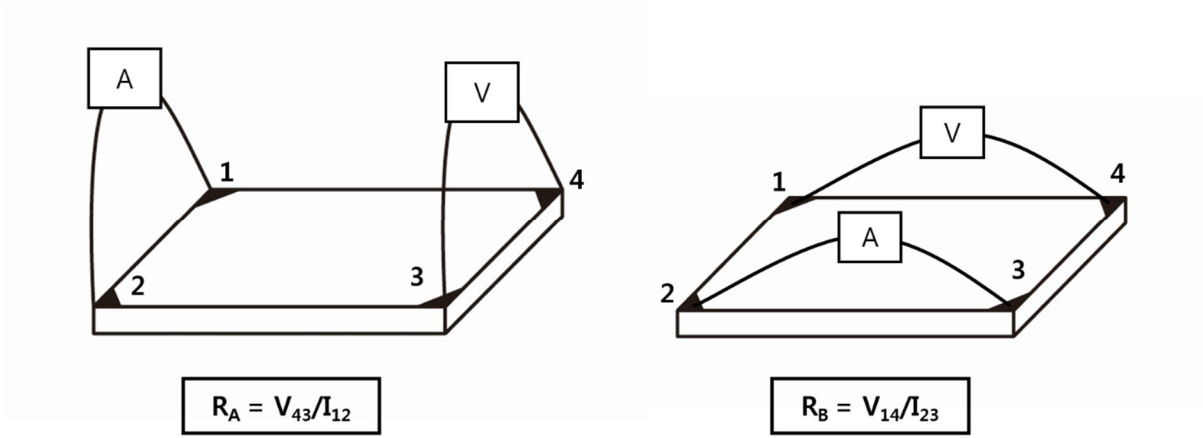


**Figure 3.** A simple mimetic diagram to illustrate the van der Pauw method. The left setup is for getting the sheet resistance measured by the vertical axis ( $R_A$ ), and the right setup is measured by the vertical axis ( $R_B$ ).

Additionally, we can calculate the whole sheet resistance ( $R_S$ ) with the sheet resistivity measured by the vertical axis ( $R_A$ ) and the sheet resistance measured by the horizontal resistivity ( $R_B$ ) via the following equation.

$$\text{Exp}(-\pi R_A/R_S) + \text{Exp}(-\pi R_B/R_S) = 1 \dots\dots\dots (2)$$

Consequently, we can also calculate the bulk resistivity ( $\rho$ ) with sample thickness ( $d$ ) and whole sheet resistance ( $R_S$ ).

$$\rho = R_S * d \dots\dots\dots (3)$$

Therefore, we can calculate the electric conductivity of the whole system using the van der Pauw method by measuring the sample resistivity.

## 2.5 Raman spectroscopy

It is an analyzing method to study about oscillation of molecule by analyzing strength of scattered light as a function of by frequency shift.

When light penetrate a medium, scattering may result, i.e. light propagates in a direction different from original direction. If also the frequency is changed, the light may be Raman scattered. The name comes from the Indian physicist who discovered the phenomenon, C.V. Raman. When he sent blue ray into solution, he firstly found this phenomenon seeing scattering of green light<sup>[30]</sup>.

If the light that is scattered retains its original energy we call it Rayleigh scattering or elastic scattering. If the scattered light has a different photon energy than the original beam, then we say that it has experienced Raman scattering or inelastic scattering. Particularly in the process of energy changing scattering, the molecules of the medium undergo a change in vibrational state, transferring energy to or from the light. The latter is called Stokes scattering, the former anti-Stokes scattering<sup>[31]</sup>.

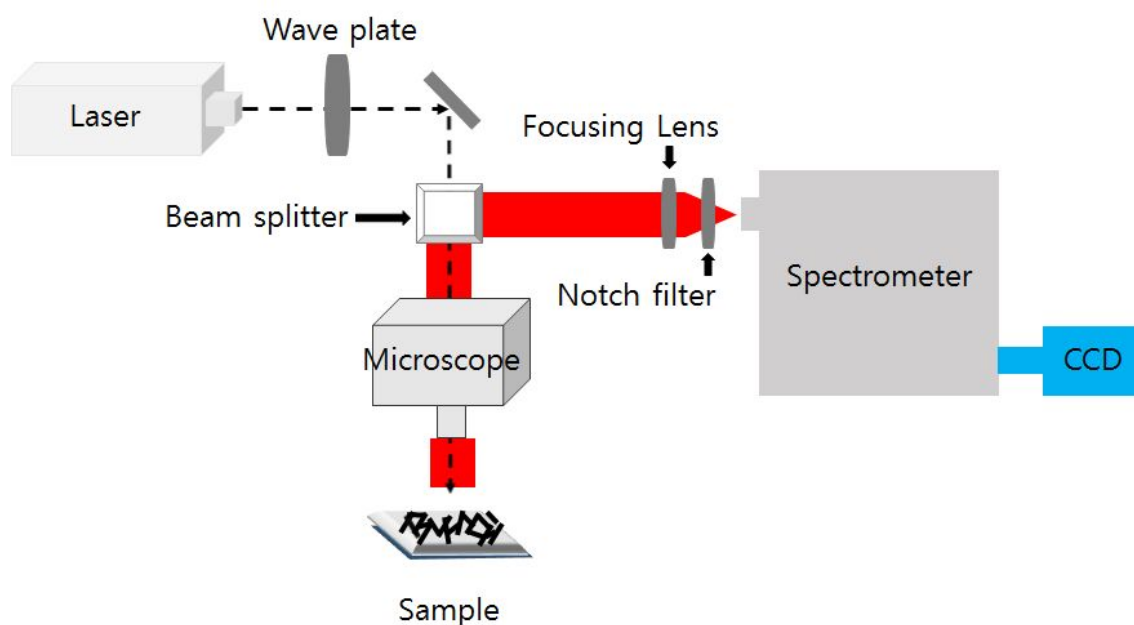
Raman-scattered light has lower energy than that of incident light since only a small fraction of the photons exchange energy with the molecules. Stokes-scattered light has longer wavelength than the incident light, reflecting the fact that it has given up some of its energy to the molecules. On the contrary, when anti-stoke effect is appeared, the scattered light has higher energy than that of incident light and shorter-wavelength light is scattered, because the scattered light contains an energy contribution from molecule<sup>[31]</sup>.

The energy exchange between light and substance, which happens during these process has close relationship with molecule structure, and the analysis of molecule structure of substance is possible

through this scattered light, because Raman scattered light has unique characteristics according by the substance.

In an experiment we analyze how much the scattered light shifted compared to Rayleigh scattering and show this as raman shift. Because the number of ground state molecule is generally more than that of molecules in excited state, the effect of stokes appeared bigger than that of anti-stokes, and it shows greater strength in spectrum.

So when analyzing Raman spectrum, stokes effect is mainly used. And when Raman spectrum was measured, the laser was illuminated in right angle to avoid radiant rays of lighting source, and the outline of set-up scheme is as scheme 2.



**Scheme 2.** The simple set-up scheme of Raman spectroscopy.

## 3. Experimental Process

### 3.1 Materials and Characterization

To make a composite of PVA with SWCNT (unidym, purified HIPCO Single-Wall Carbon Nanotube, purified 5 wt %  $\leq$  impurities  $\leq$  15 wt % ash content) , polyvinyl alcohol (PVA, Mw 146,000–186,000, 87–89 hydrolyzed, ALDRICH) was dissolved in distilled water. Solutions of hexadecyl trimethyl ammonium bromide (CTAB, 99%, MW= 364.45, Acros) and SDBS (Dodecylbenzenesulfonic acid, sodium salt, 88%, MW = 348.48, Acros) were used to make the CNT dispersion. In addition, we ultra-sonicated using a tip sonicator (Hielscher ultrasonics GmbH, UIS250L) at 60% amplitude and 0.5 cycle for the CNT dispersion.

The CNT dispersion and PVA–CNT composite film was characterized by a field emission scanning electron microscope (FE-SEM, Hitachi S-4800), UV/VIS spectrometer (Lambda 35, PerkinElmer), Optical Microscope (Nikon ECLIPSE LV100D-U), and Dynamic Light Scattering (DLS, Microtrac, nanotracs wave NPA 150). Raman spectra were taken with a micro Raman system (ACRON, UniNanotech, Korea). The excitation source was a 532 nm laser (2.33 eV). The film thickness was measured by an Alpha-Step IQ surface profiler (KLA tencor). The electric properties were measured using a Keithley 236 Source measure unit.

## 3.2 Process of CNT dispersion

To define the optimum initial CNT dispersion, we first used each SDBS and CTAB surfactant to find an appropriate surfactant. We then analyzed the degree of dispersion based on each concentration of CNT, and the sonication time.

To manufacture a well-dispersed CNT dispersion, we set up the initial SWCNT concentration at 0.001 g/ml to 0.002 g/ml and dispersed it with 1 ml distilled water, adding either SDBS or CTAB surfactant. Finally, we determined the optimum concentration via optical microscope and determined the effect of the surfactant type.

In addition, during the study of CNT dispersion, When we disperse a CNT suspension, we find that the CNT aggregation size differed greatly from our expectations following the sonication time dependence. This means that the sonication time is a critical factor for the dispersion, so we analyzed it to check for the aspect of transition following the sonication time dependence. To minimize the surfactant effect and clarify the sonication time effect, 0.002g of each kind of surfactant was used. The sonication time had a 10 min interval, and sonication was conducted at 10 min, 20 min, 30 min, 40 min, 50 min, and 60 min and characterization was performed via optical microscope.

However, although we can determine the optimum sonication time via these steps, it has some aggregations; as such, we can introduce the centrifuge step to get rid of large aggregations.

Centrifugation was conducted at 2000 rpm for 5 minutes. After that, the supernatant was separated and the real concentration of CNT dispersion could be calculated. To get this information, we used the optical absorbance spectra and calculated the real concentration by following the Lambert–Beer law.

$$A = \log \frac{I_0}{I} = \epsilon c l$$

Following the Lambert–Beer law, absorbance (A) can be calculated by a logarithm with an intensity ratio of detected light and initial light; it is the same value, which multiplies the extinction coefficient ( $\epsilon$ ), concentration of CNT suspension (C), path length of sample (l)

We calculated the concentration after centrifuging the samples, by getting the absorbance values and the different series concentration of SWCNT suspension. At the end of this step, we can get the extinction coefficient ( $\epsilon$ ) values for before and after the centrifuged SWCNT suspension. Through the ratio of the extinction coefficient before and after the centrifuged SWCNT suspension, we assume the real concentration after centrifuging the SWCNT suspension.

In addition, the optical absorbance spectra information can be used to determine the effect of the surfactant.

### 3.3 PVA–CNT composite and fabrication film

Through the experiment about making a CNT suspension in which aggregation has been eliminated, we get a clean CNT suspension. We then mix together 2wt% PVA solution and CNT suspension to fabricate a PVA–CNT composite.

Even though we succeed in making a clear pure CNT suspension, when we added the PVA solution, we can check that coagulation has occurred.

Thus, to try to solve this problem, we conducted additional sonication after mixing a CNT suspension and PVA solution together, and we found appropriate additional sonication time. Additionally, the PVA solution and CNT suspension mixing was conducted at 400 rpm for 5 minutes. After mixing via stirring, we conducted additional sonication following time dependence to optimize the additional sonication time.

Finally, we successfully made a PVA–CNT composite solution following these steps. Then, to make a PVA–CNT composite film, we used the drop casting method. A film was made using the PVA–CNT composite mass ratio dependence. The ratios were 1:10, 1:5, 1:2, 1:1, 2:1, 5:1, and 10:1, and all samples were made on an Si wafer with an oxide coating, and 20  $\mu$ l of each sample was used.

### 3.4 Electric properties PVA–CNT composite film

For measuring electric conductivity PVA–CNT composite film, we used the van der Pauw method. After making a PVA–CNT composite film on SiO<sub>2</sub>, we then set up an ohmic contact electrode, as shown in Figure 4.

Next, we calculated the sheet resistance for each axis. ( $R_A = V_{43} / I_{12}$ ,  $R_B = V_{14} / I_{23}$ ) Finally, we were able to calculate the whole sheet resistance by following this equation.

$$\text{Exp}(-\pi R_A / R_S) + \text{Exp}(-\pi R_B / R_S) = 1$$

Following these steps, we were able to calculate the whole sheet resistance ( $R_S$ ) and could calculate the bulk resistivity by the whole sheet resistance ( $R_S$ ) multiplied by the thickness. In this way, we can get the electric conductivity of the film via the reciprocal resistivity.

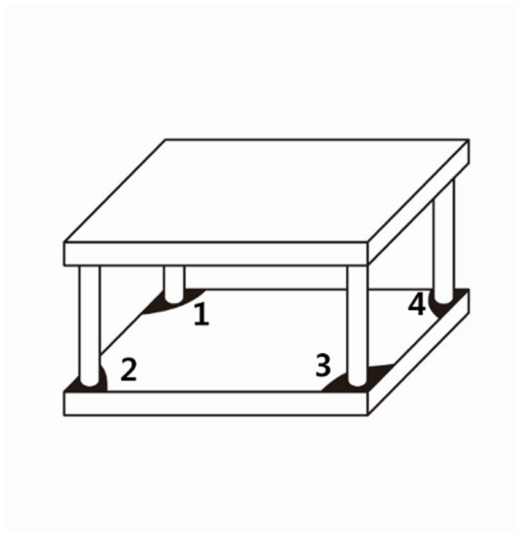


**Figure 4.** Electrode set up for measuring the electric conductivity via the van der Pauw method.

## 4. Result and Discussion

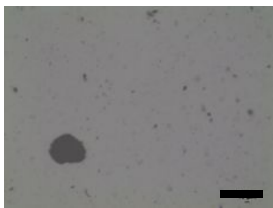
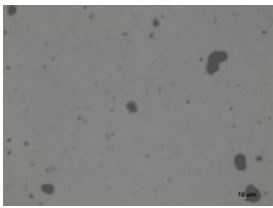
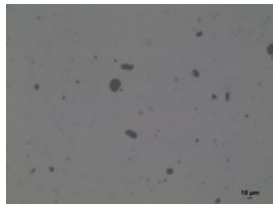
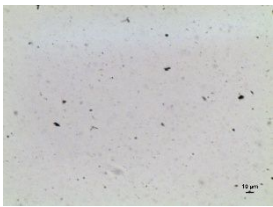
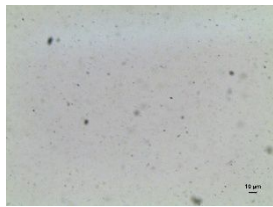
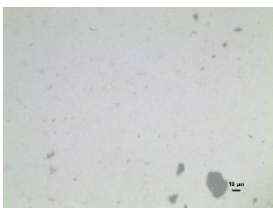
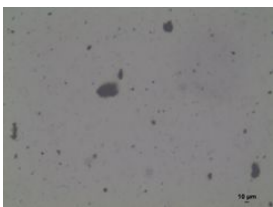
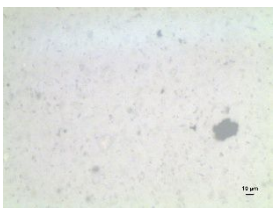
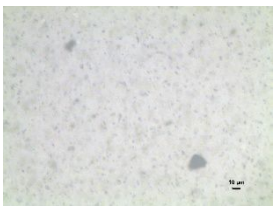
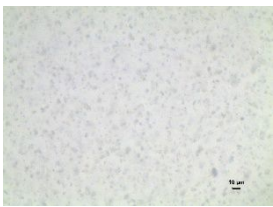
### 4.1 SWCNT dispersion

To optimize the CNT dispersion condition, we analyzed the optical characterization of each sample. We set up our samples as follows in Table 1. We identified that the 1 mg/ml CNT was well dispersible; however, it is also interesting to see if we could manage greater CNT dispersion. Therefore, we also tried to disperse 2 mg/ml CNT. Then, we checked how to change the differing sonication time dependence.

Surfactant	Surfactant concentration	CNT concentration
CTAB	2 mg/ml	1 mg/ml CNT
	4 mg/ml	1 mg/ml CNT
	10 mg/ml	1 mg/ml CNT
	4 mg/ml	2 mg/ml CNT
	8 mg/ml	2 mg/ml CNT
	20 mg/ml	2 mg/ml CNT
SDBS	2 mg/ml	1 mg/ml CNT
	4 mg/ml	1 mg/ml CNT
	10 mg/ml	1 mg/ml CNT
	4 mg/ml	2 mg/ml CNT
	8 mg/ml	2 mg/ml CNT
	20 mg/ml	2 mg/ml CNT

**Table 1.** List of conditions for CNT concentration and kind of surfactant and surfactant concentration.

In these experimental conditions, we could see that the 2 mg/ml CNT suspension has greater aggregation than the 1 mg/ml over the same sonication time. It means that regardless of the surfactant amount, they have a limited dispersion state. Therefore, to optimize the dispersion state, we chose the 1 mg/ml CNT condition and checked the difference with the surfactant amount and the sonication time dependence.

CNT suspension condition	Sonication time		
	20 min	40 min	60 min
1 mg/ml CNT +SDBS 2 mg/ml			
1 mg/ml CNT +SDBS 4 mg/ml			
1 mg/ml CNT +SDBS 10 mg/ml			
1 mg/ml CNT +CTAB 2 mg/ml			
1 mg/ml CNT +CTAB 4 mg/ml			
1 mg/ml CNT +CTAB 10 g/ml			

**Figure 5.** CNT dispersion state for the corresponding surfactant condition and sonication time dependence. (The scale bar corresponds to 50  $\mu\text{m}$ )

We show, as in Figure 5, that we succeeded in showing that a sonication time of over 40 min makes little difference to the dispersion state. Moreover, when the sonication time was longer than 60 min, they tended to create much smaller CNT aggregation, but also created aggregation with diameters of over 1  $\mu\text{m}$ . This means that the dispersion effect still exists; however, it creates re-aggregation and makes larger particles at the same time, as shown in Figure 6, which shows the DLS data. Consequently, we can conclude that over 60 min of sonication has no effective for the quality of CNT dispersion.

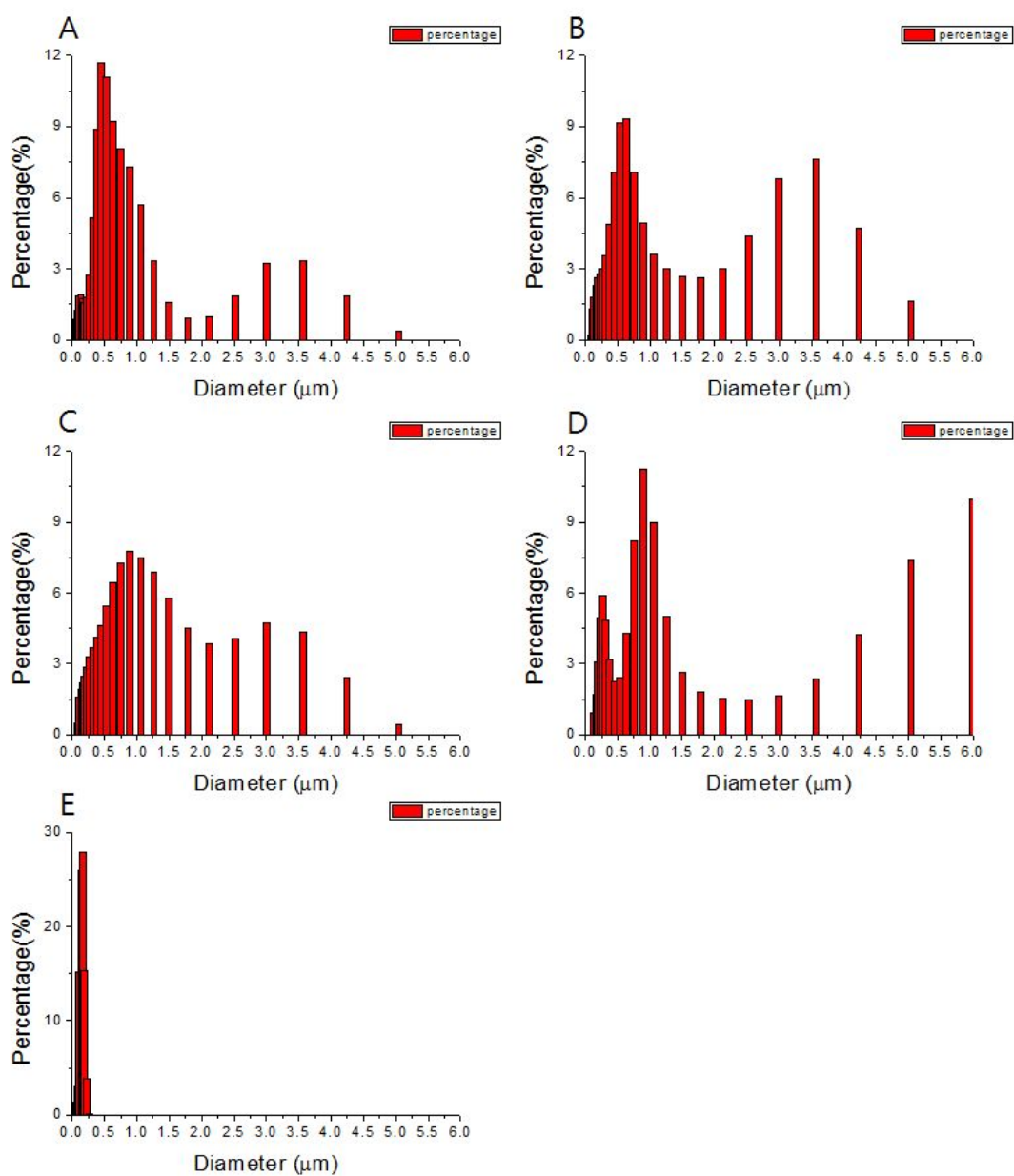


**Figure 6.** 1 mg/ml CNT with 10 mg/ml CTAB surfactant suspension distribution of particle size, following the sonication time dependence by DLS. (A) 30 min sonication (B) 60 min sonication (C) 90 min sonication (D) 120 min sonication (E) particle distribution of only 10 mg/ml CTAB with water solvent.

In this step, we can determine that one of important factor of the CNT dispersion is the sonication time. Most research found that a long sonication time can damage CNTs<sup>[32],[33]</sup>. It also can give the low electrical properties of SWCNT. Therefore, to avoid CNT damage, we set up the sonication time at under 60 min, and we checked the damage of the pristine SWCNT. For the specification of how the sonication time affects the SWCNT dispersion, we tried to check the film morphology with 40 min sonicated SWCNT samples and 180 min sonicated SWCNT samples, compared by Raman D and G bands of each samples.

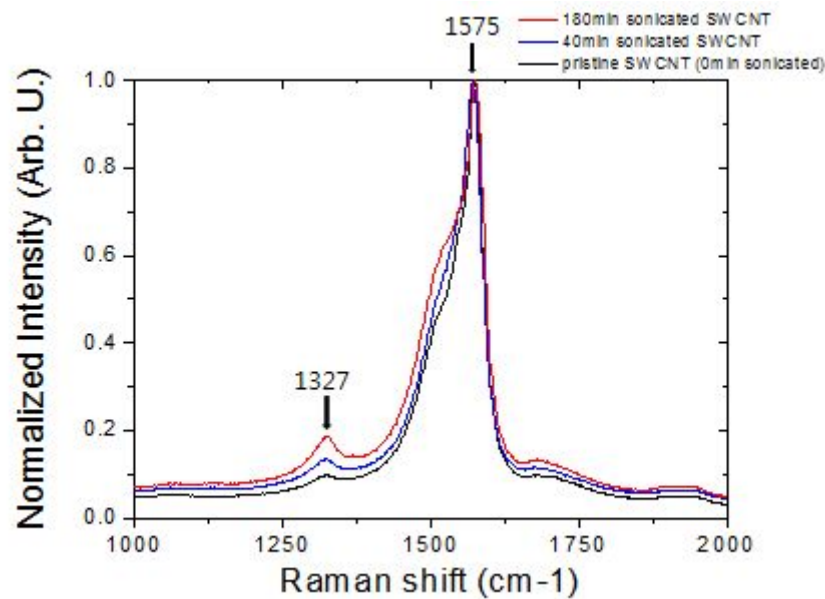


**Figure 7.** Raman D bands ( $1327\text{ cm}^{-1}$ ) and G bands ( $1575\text{ cm}^{-1}$ ) of SWCNT following different sonication time. The more sonication time lead to increase D peak intensity. D peak intensity increase following orders (pristine SWCNTs (black line) < 40 min sonicated SWCNT (blue line) < 180 min sonicated SWCNT (red line))

Following Figure 7, we can confirm the SWCNT damage after a long sonication time via Raman spectroscopy. It is also proved in a study by Wepasnick et al<sup>[33]</sup>. Carbon materials that have an  $sp^2$

bond form show Raman bands roughly around 1350 and 1580  $\text{cm}^{-1}$ : the D and G bands, respectively. The D-band is related to CNT damage. Normally, the G-band contains information relating to the geometric structure, because it is sensitive to strain effects in  $\text{sp}^2$  nanocarbons. In addition, the D-band gives information that characterizes the disorder in  $\text{sp}^2$  carbon materials<sup>[34]</sup>.

In addition, we checked that the 10 mg/ml surfactant concentration had the best dispersion state. It can be seen through an Optical Microscope; however, in the case of a CTAB surfactant, there are an excess of crystalized surfactant on room temperature, because the surfactant solubility is lower than 1wt% at room temperature<sup>[35]</sup>. Therefore, we used the optical absorbance of each suspension to determine the degree of dispersion, as shown in Figure 8.

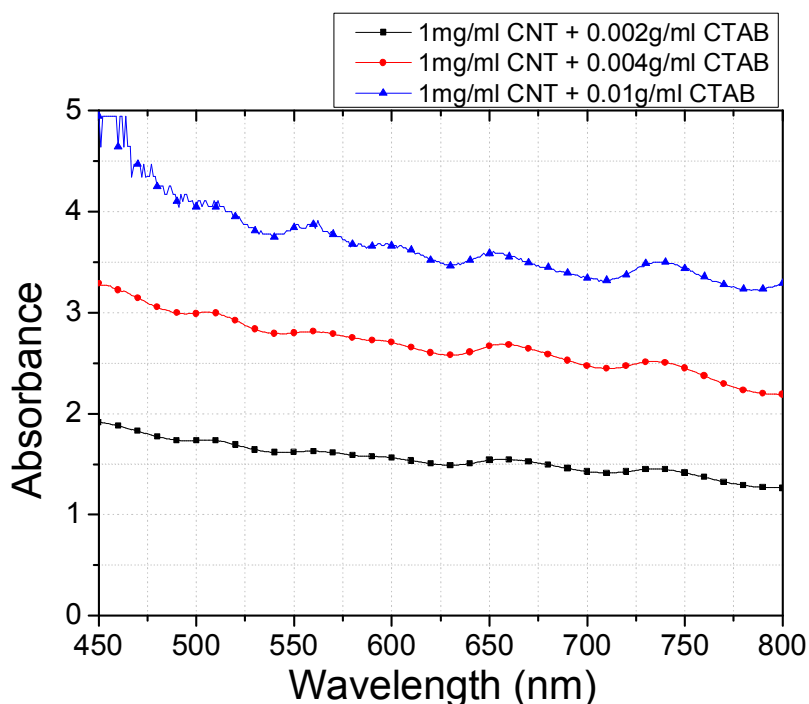


**Figure 8.** Optical spectra series of dispersed CNT suspension from different CTAB surfactant amount 2 mg/ml to 10 mg/ml.

In Figure 8, the CNT amount is a constant 1 mg in a 1 ml solvent; however, as waves get higher, the absorbance values are followed by increasing the surfactant amount. It means that a suspension that has more surfactant absorbs more light than one that has less. Naturally, it can be said that a suspension that has a higher absorbance has much better dispersed CNT particles than a suspension that has less absorbance. Because the aggregated CNT particles have sedimentation on the bottom. Moreover, the absorbance of surfactant on its own was also considered, but this effect is very subtle for the whole absorbance.

In terms of these things, we can conclude that 1 mg/ml CNT with a 10 mg/ml CTAB surfactant suspension is better dispersed than a 1 mg/ml CNT with 2 mg/ml CTAB surfactant suspension.

Additionally, we find that both CTAB and SDBS surfactant, which play a role in anion surfactants and cation surfactants have no big difference in their dispersion state at the same surfactant amount, as shown Figure 9.

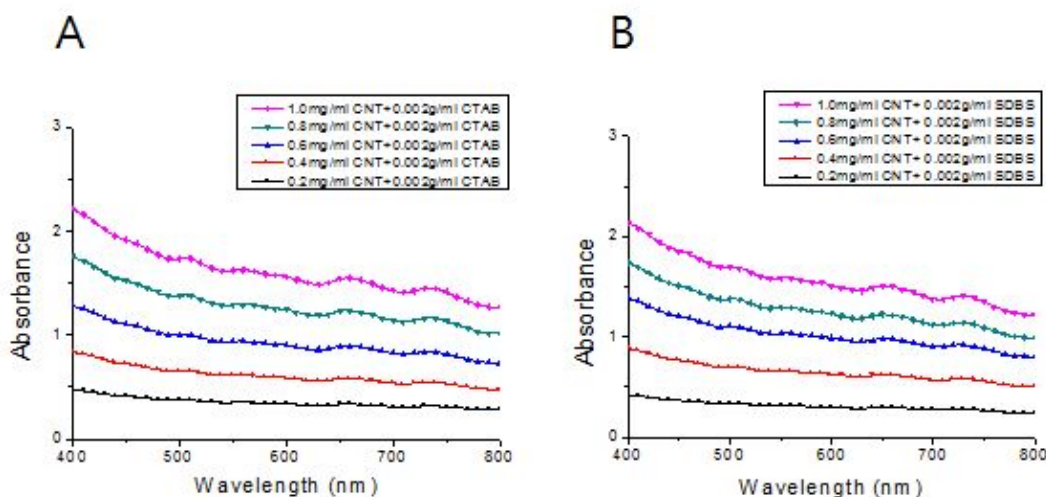


**Figure 9.** Optical spectra series of dispersed CNT suspension from different kinds of surfactant. (A) 0.2–1.0 mg/ml CNT concentration dispersion with 2 mg/ml CTAB (B) 0.2–1.0 mg/ml CNT concentration dispersion with 2 mg/ml SDBS

However, in the case of CTAB surfactants, research shows that they have a well dispersed state below its Krafft temperature<sup>[36]</sup>. In this research, that is not considered, but it is possible and has potential for better electrical properties below the Krafft temperature dispersion state. For this reason, we focused on CTAB than SDBS surfactant for dispersion.

After setting up the proper sonication time and surfactant condition, we dispersed the CNT suspension via centrifugation to get rid of the remaining large aggregations and surfactant to make the sanitation supernatant after centrifuging. The centrifuge condition was 2000 rpm at 12 °C for 5 minutes. The well-made supernatant had no larger aggregation than before.



**Figure 10.** Supernatant of SWCNT 1 mg/ml with CTAB surfactant 10 mg.

As shown in Figure 10, the supernatant of the SWCNT suspension has a decreased quantity of large aggregated particles compared to before due to centrifugal force, and it has decreased remaining CTAB particles floating in suspension. Finally, there remain small and well dispersed CNT particles. It can be determined by comparing with Figure 5. Through this step, we can get a clearer SWCNT suspension than before centrifugation.

In addition, due to using a centrifuge to get the supernatant, the CNT amount was decreased compared to the initial state. Therefore, to measure the exact CNT amount in suspension, we analyzed the visible light absorbance. Through this step, we can calculate the exact CNT concentration after centrifuged suspension via the Lambert–Beer law. As shown Figure 11, the CNT concentration has approximately 3% loss compared to before the centrifuged CNT suspension. The well-dispersed suspension has a very stable state, thus the very little sedimentation has occurred in the CNT aggregation.

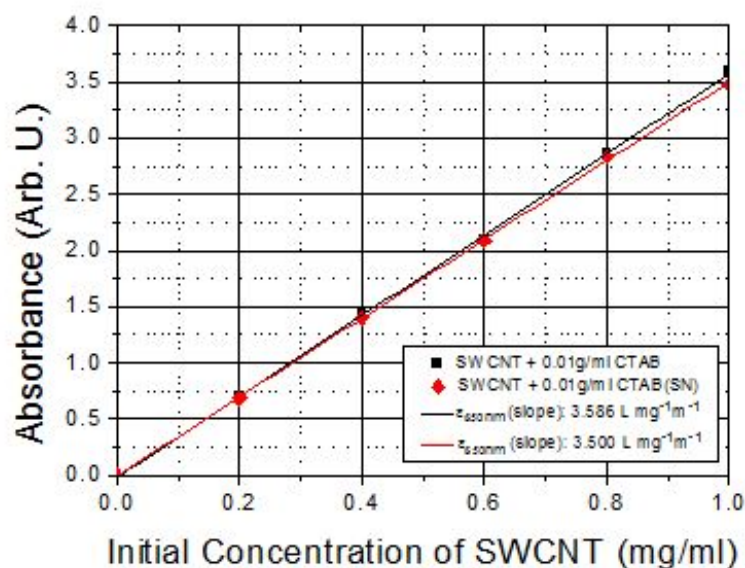


**Figure 11.** Visible light absorbance of the CNT suspension following concentration dependence in at 650 nm wavelength. (C) 1 mg/ml CNT suspension with 1 wt% CTAB surfactant.

## 4.2 PVA–CNT composite and fabrication film

We used a well-dispersed CNT suspension and made a composite with the PVA solution. We have successfully made the suspension; however, when they were mixed together, they result in aggregate. This phenomenon can occur due to various factors; however, the prime factor is the interaction of PVA and CNT. Since the stability of colloidal dispersions has an effect on the addition of macromolecules such as polymers. The adsorption of macromolecules on the particle surfaces results in an aggregation process<sup>[37],[38]</sup>. The reason can be, for instance, the bridging of multiple CNTs by a single PVA molecule, when one of the long and flexible polymer chains makes contact with several nanotubes and thus brings them together into an aggregate. Another possibility is that the aggregation is triggered by the stabilizing CTAB molecules, leaving the CNT surfaces in favor of the PVA, but we could not investigate this question in more detail within the scope of this thesis.

Thus, to optimize the dispersion state, we tried additional tip sonication after mixing, which was conducted for 5 minutes at 400 rpm. We also used additional sonication with 30 min intervals for checking the aspect of transition, and we found that when the stirring time was longer, there was much greater aggregation, due to the increased collision chance among the CNT particles with PVA. Therefore, we maintained the stirring time at 5 minutes for mixing the PVA–CNT composite solution.

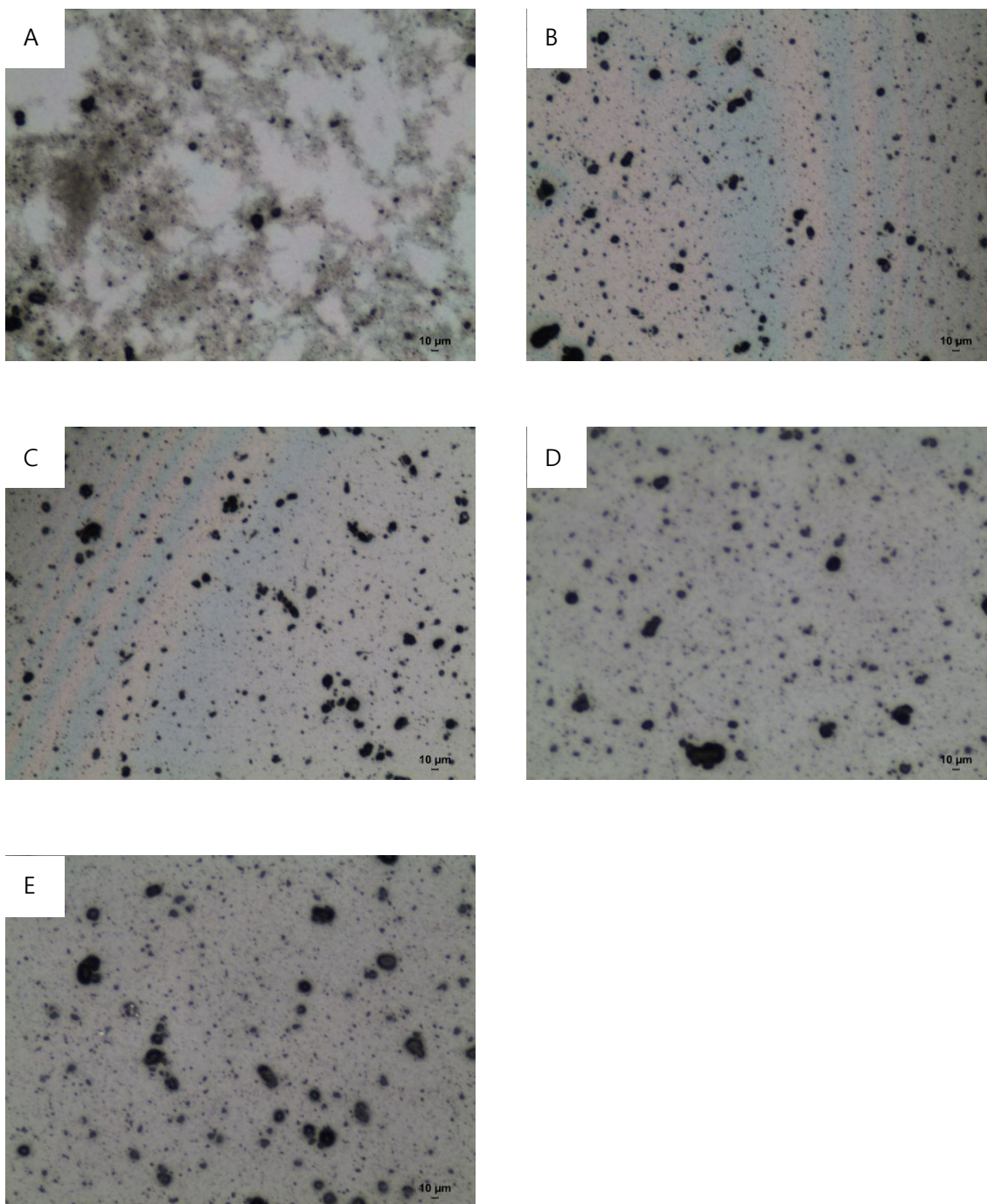


**Figure 12.** Optical microscope image of the dried PVA–CNT composite solution following sonication time dependence after mixing. (A) 0 min sonication (just 5 min stirring) (B) 30 min sonication (C) 1 hour sonication (D) 1.5 hour sonication (E) 2 hour sonication.

After mixing and additional sonication, the additional sonication time made large aggregations rapidly. It means that additional sonication has no merit for the dispersion, rather it seems best when mixing PVA solution and CNT suspension immediately after a just under 5 min stirring condition. Until 30 min after sonication, there was no big difference; however, there was much coagulation after the sonication time dependence of over 30 min. It means that longer after sonication has no effect for the dispersion of the mixture; rather, longer sonication creates a worse dispersion state and triggers aggregation. Next, a PVA–CNT composite film was made using the composite solution 20  $\mu$ l on a SiO<sub>2</sub> wafer via the drop-casting method. In addition, we checked the morphology of the PVA–CNT composite film via SEM imaging. Each sample had 1:10, 1:5, 1:1, 5:1, or 10:1 PVA–CNT mass ratio.

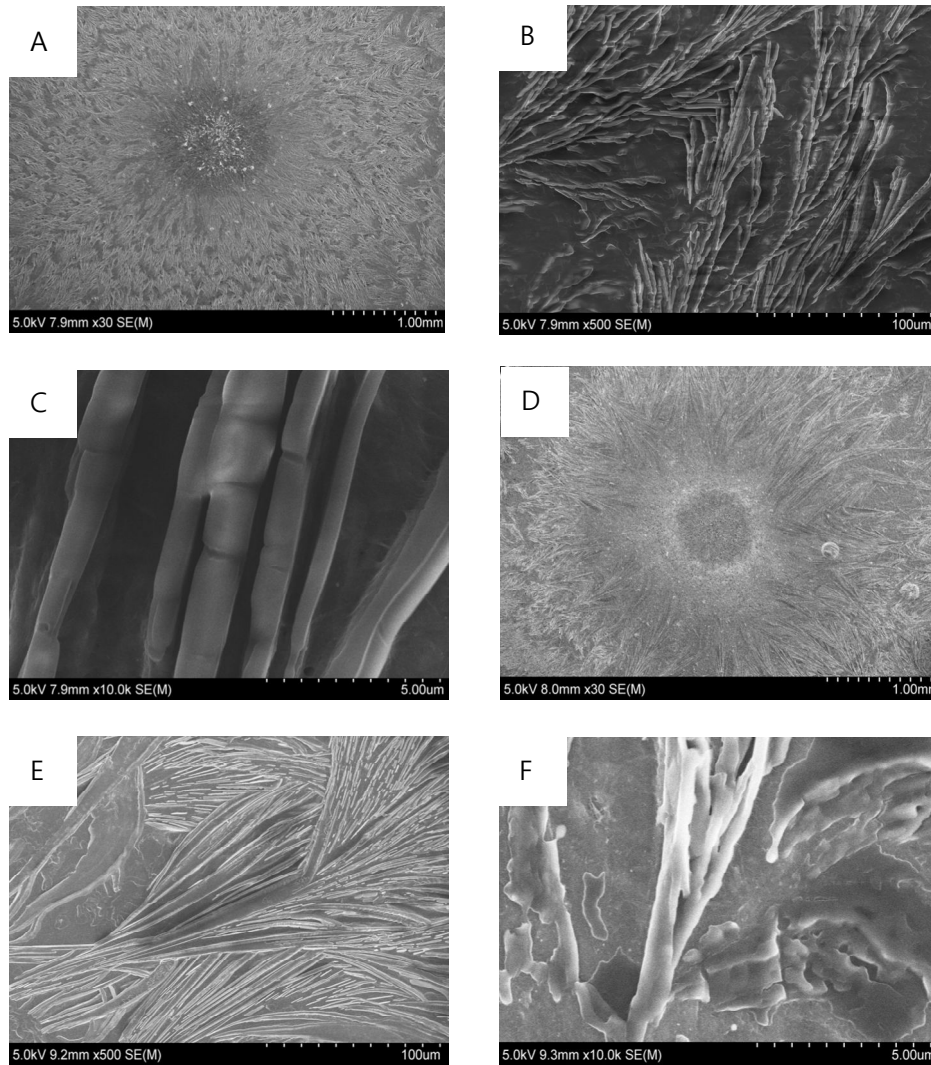


**Figure 13.** SEM images of the PVA–CNT composite film morphology. (A) Whole image of PVA–CNT 1:10 mass ratio film. (B) Enlarged CNT branch part. (C) Enlarged B image. (D) Whole image of the PVA–CNT 1:5 mass ratio film. (E) Enlarged CNT branch of PVA–CNT 1:5 mass ratio. (F) Enlarged E image.

We checked the PVA–CNT film samples that had mass ratios 1:10 and 1:5 via SEM images. The group of SEM images showed in Figure 13. Composite film that has a CNT-dominated condition has a similar surface morphology to CNT film via the drop-casting method. The PVA/CNT interaction is

strong, but the PVA amount is very subtle. Thus, the film shape is similar to the CNT shape. When the PVA amount was increased (Fig 13 (B),(C)), the CNT branch seemed coated by more PVA. However, the CNT branch shape still is dominant. The PVA mass increases more, and the PVA–CNT ratio was 1:1, 5:1, and 10:1. For our samples, they have similar surface morphologies with the only PVA film surface, as shown in Figure 14.

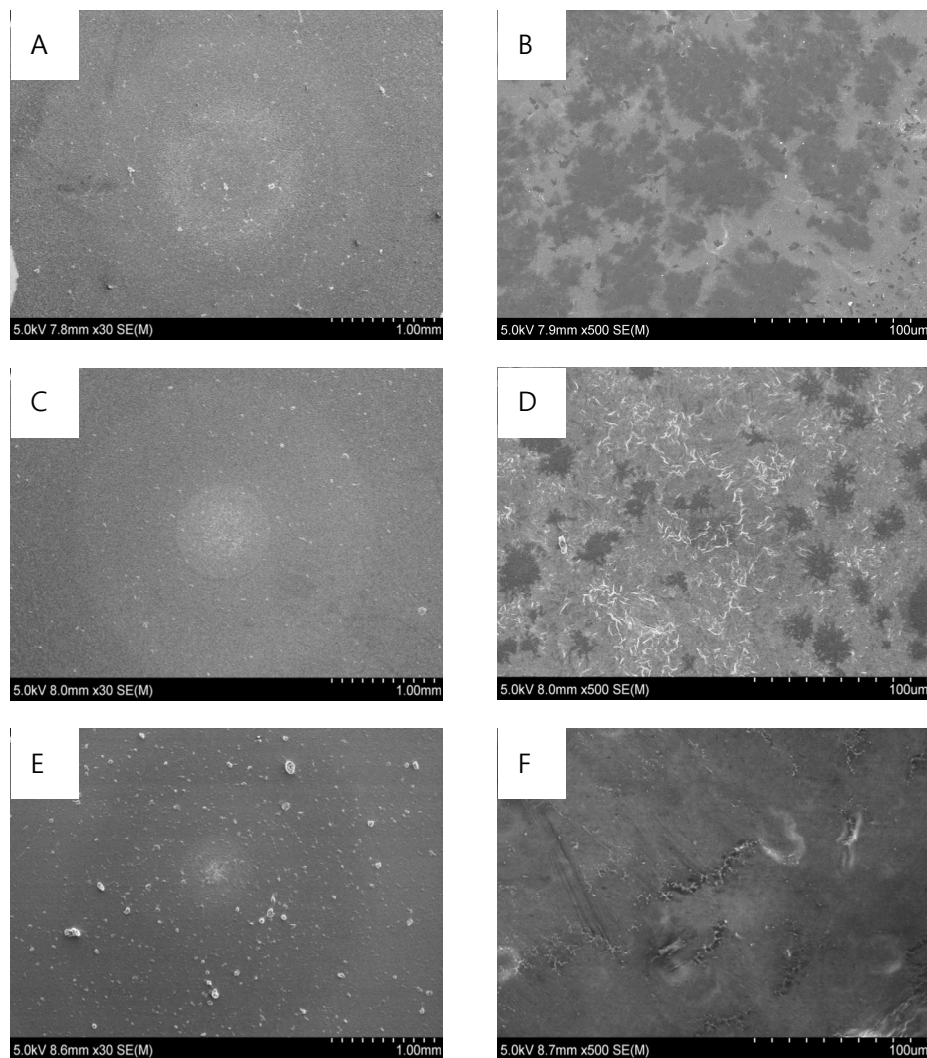


**Figure 14.** SEM image of the PVA–CNT composite film morphology. (A) Image of PVA–CNT 1:1 mass ratio film. (B) Image A enlarged. (C) Image of PVA–CNT 5:1 mass ratio film. (D) Image B enlarged. (E) Image of PVA–CNT 10:1 mass ratio film. (F) Image E enlarged.

### 4.3 Electrical properties of the PVA–CNT composite film

To measure the electrical properties of the PVA–CNT composite film, we prepared each composite sample following the mass ratio difference. We used 2 wt% PVA solution and 1 mg/ml SWCNT suspension, then mixed it to the considered mass ratio. The composite film was made on SiO<sub>2</sub> Wafer, and a 20 µl composite solution was used for all samples. Each mass ratio was set up as shown in Table 2.

PVA solution	CNT suspension	PVA–CNT Mass Ratio
5 µl	1 ml with 1 mg SWCNT	1:10
6.25 µl	1 ml with 1 mg SWCNT	1:8
10 µl	1 ml with 1 mg SWCNT	1:5
25 µl	1 ml with 1 mg SWCNT	1:2
50 µl	1 ml with 1 mg SWCNT	1:1
100 µl	1 ml with 1 mg SWCNT	2:1
250 µl	1 ml with 1 mg SWCNT	5:1
400 µl	1 ml with 1 mg SWCNT	8:1
500 µl	1 ml with 1 mg SWCNT	10:1

**Table 2.** Conditions for making the PVA–CNT composite solution.

Conductivity was measured by the van der Pauw method. Before the whole resistivity was calculated, we got 4 I–V curves that applied each axis per sample to check the sheet resistance and repeat for the prepared kinds of PVA–CNT composite, and calculated the sheet resistance via the van der Pauw equation.

Next, we multiplied the sample thickness by the sheet resistance, then we were finally able to get each sample's conductivity via the reciprocal of resistivity.

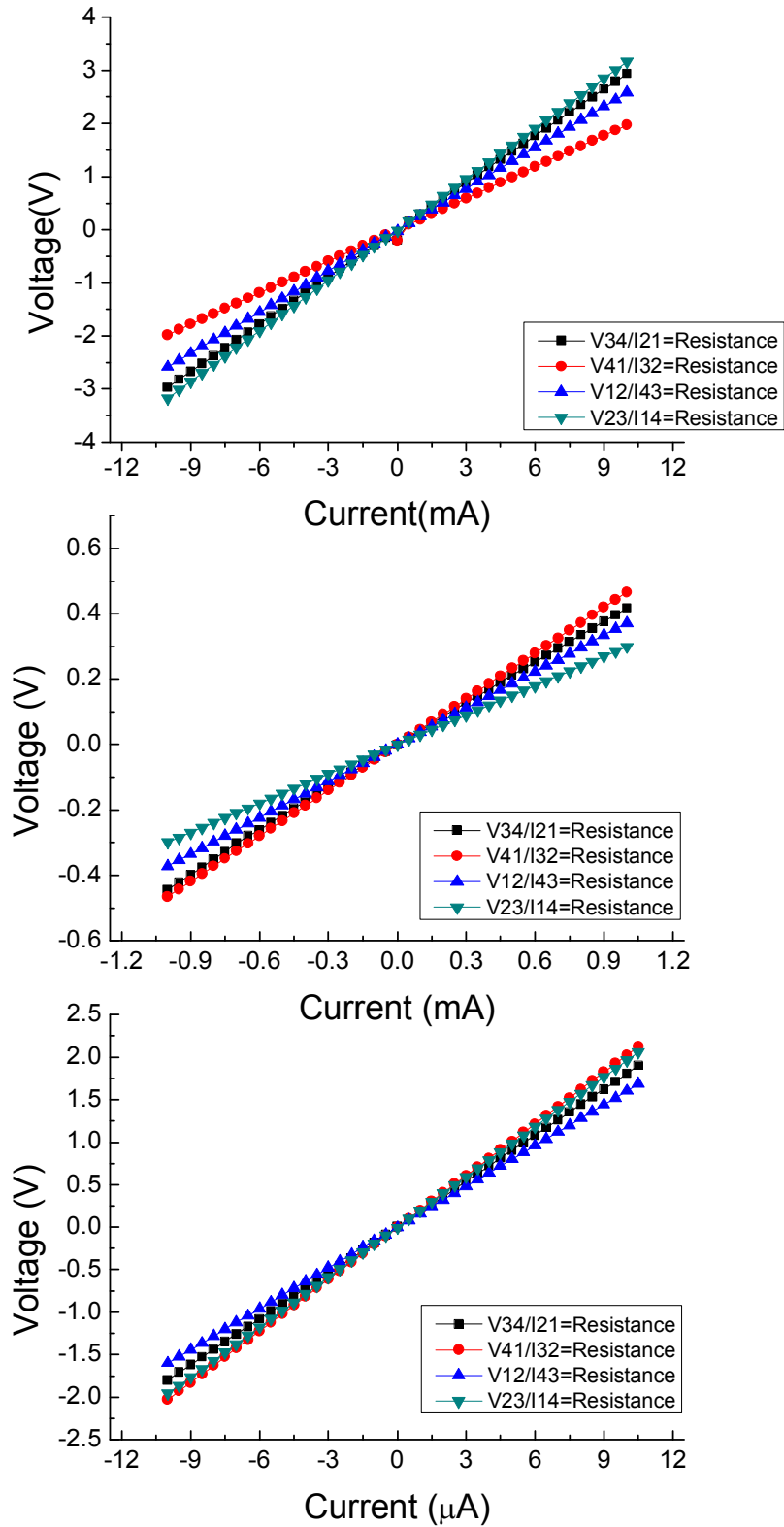


**Figure 15.** I-V curves when applying current each axis measured by van der Pauw method. (A) I-V curves of PVA-CNT 1:5 mass ratio. (B) I-V curves of PVA-CNT 1:1 mass ratio. (C) I-V curves of PVA-CNT 5:1 mass ratio

As shown Figure 15, each I-V curve shows that the ohmic conducting system all of axes when applying the current for each sample. The geometric difference or partially localized CNT makes some error for the I-V curves. In addition, when the PVA amount was dominant compared to the CNT amount, each slope's value was higher than the CNT-dominant condition. This is because PVA has a high resistivity and can make a harder conducting path than in the CNT dominant condition.

For calculating the whole resistivity, we calculated the sheet resistance. Values are listed Table3.

PVA-CNT mass ratio	$R_1$ ( $V_{34}/I_{21}$ )	$R_2$ ( $V_{41}/I_{32}$ )	$R_3$ ( $V_{12}/I_{43}$ )	$R_4$ ( $V_{23}/I_{14}$ )	$R_A$ ( $R_1+R_3$ )/2	$R_B$ ( $R_2+R_4$ )/2
1:10	$1.283 \cdot 10^2$	$1.9731 \cdot 10^2$	$1.3517 \cdot 10^2$	$1.13 \cdot 10^2$	$1.317 \cdot 10^2$	$1.551 \cdot 10^2$
1:8	$1.5309 \cdot 10^2$	$1.3392 \cdot 10^2$	$1.2841 \cdot 10^2$	$1.5849 \cdot 10^2$	$1.407 \cdot 10^2$	$1.462 \cdot 10^2$
1:5	$2.9551 \cdot 10^2$	$1.9768 \cdot 10^2$	$2.5835 \cdot 10^2$	$3.1733 \cdot 10^2$	$2.769 \cdot 10^2$	$2.575 \cdot 10^2$
1:2	$2.2334 \cdot 10^2$	$2.2337 \cdot 10^2$	$3.5058 \cdot 10^2$	$3.0118 \cdot 10^2$	$2.869 \cdot 10^2$	$2.622 \cdot 10^2$
1:1	$4.293 \cdot 10^2$	$4.6614 \cdot 10^2$	$3.7212 \cdot 10^2$	$2.9923 \cdot 10^2$	$4.007 \cdot 10^2$	$3.826 \cdot 10^2$
2:1	$6.3154 \cdot 10^3$	$5.7178 \cdot 10^3$	$2.0409 \cdot 10^3$	$6.5479 \cdot 10^3$	$4.178 \cdot 10^3$	$6.132 \cdot 10^3$
5:1	$1.8028 \cdot 10^5$	$2.0302 \cdot 10^5$	$1.603 \cdot 10^5$	$1.9651 \cdot 10^5$	$1.7029 \cdot 10^5$	$1.997 \cdot 10^5$
8:1	$4.313 \cdot 10^7$	$4.1671 \cdot 10^7$	$4.5506 \cdot 10^7$	$3.2448 \cdot 10^7$	$4.4318 \cdot 10^7$	$4.2079 \cdot 10^7$
10:1	$2.4679 \cdot 10^7$	$6.2445 \cdot 10^6$	$2.115 \cdot 10^7$	$1.0899 \cdot 10^8$	$2.2914 \cdot 10^7$	$5.7617 \cdot 10^7$

**Table 3.** Sheet resistance of PVA-CNT composite film with different axis current applying.

After getting the sheet resistances  $R_A$  and  $R_B$ , which were measured with different axes, we calculated a more accurate sheet resistance  $R_S$  with  $R_A$  and  $R_B$  by the van der Pauw equation. Next, we got the bulk resistivity via multiplying the  $R_S$  and the film thickness. The film thickness is measured by the surface profiler alpha-step. The values are listed Table 4.

PVA–CNT mass ratio	$R_s(\Omega)$	d (thickness, cm)	bulk resistivity ( $\Omega \cdot \text{cm}$ )	conductivity (S/cm)
1:10	$0.65 \cdot 10^3$	$8.0 \cdot 10^{-4}$	$5.2 \cdot 10^{-1}$	1.923
1:8	$0.65 \cdot 10^3$	$9.0 \cdot 10^{-4}$	$5.85 \cdot 10^{-1}$	1.709
1:5	$1.21 \cdot 10^3$	$7.4 \cdot 10^{-4}$	$8.95 \cdot 10^{-1}$	1.117
1:2	$1.24 \cdot 10^3$	$9.3 \cdot 10^{-4}$	$11.53 \cdot 10^{-1}$	0.867
1:1	$1.77 \cdot 10^3$	$7.0 \cdot 10^{-4}$	$12.39 \cdot 10^{-1}$	0.807
2:1	$2.31 \cdot 10^4$	$9.3 \cdot 10^{-4}$	$2.15 \cdot 10^1$	$4.65 \cdot 10^{-2}$
5:1	$8.37 \cdot 10^5$	$13.6 \cdot 10^{-4}$	$1.14 \cdot 10^3$	$8.77 \cdot 10^{-4}$
8:1	$1.839 \cdot 10^8$	$13.8 \cdot 10^{-4}$	$2.537 \cdot 10^5$	$3.941 \cdot 10^{-6}$
10:1	$1.7011 \cdot 10^8$	$14.0 \cdot 10^{-4}$	$2.381 \cdot 10^5$	$4.199 \cdot 10^{-6}$

**Table 4.** Bulk resistivity and conductivity of the PVA–CNT composite film.

As shown in Table 4, conductivity decreases occurred rapidly at the PVA–CNT mass ratio of 2:1 to 8:1. Thus, we can assume that making a conducting path drastically occurred in this section. Based on these results, we can try to get the percolation threshold by the logarithm of the conductivity curve. This is shown in Fig 16.

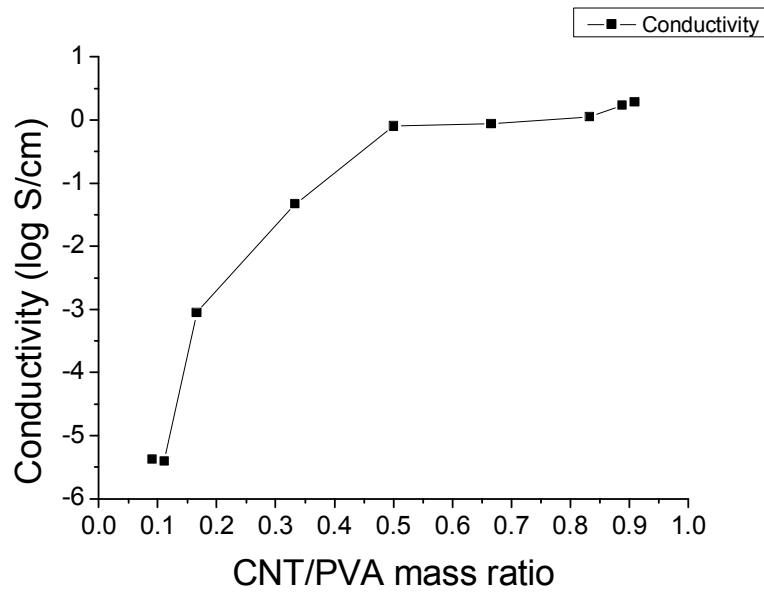


**Figure 16.** Conductivity of the PVA–CNT composite films. “0” means only PVA material, and “1” means only CNT material in the x-axis.

As shown in Fig 16, conductivity was rapidly increased from 1:8 CNT–PVA mass ratio. This means that the percolation of CNT was approximately made at the CNT–PVA mass ratio of 1:8. This value is a little higher than the normally-known percolation concentration of CNT–polymer composites, and we assume some reason for this phenomenon. First, the CNT dispersion has limitations for extremely high dispersion conditions. Next, due to the introduction of surfactants, the conductivity tended to decrease, since the reaction of the CNT-surface with the surfactant hindered the formation of the percolation model from contact with the CNT.

## 5. Conclusion

In conclusion, we manufactured the composite film which has conductivity by composing PVA and CNT. And we found out section in which conductivity changes sharply by adjusting composite mass ratio of PVA and CNT, and presumed percolation point through this, and figured out that sharp increasement of conductivity happened at the moment weight percent of CNT on PVA is 12.5%

CNT substance easily forms aggregation by each other's van der waals force in the solvent system. So in this study, the problems in dispersion were solved out as much as we could by removing left aggregation particles through centrifugal process after first dispersion by adopting surfactant and adjusting sonication condition. And it was confirmed that the effect of dispersion declined and CNT substance is damaged at same time if sonication time exceeds proper duration. So the dispersion condition was optimized by proper adjusting of ultrasound power and time.

The composite solution was produced by mixing well dispersed CNT suspension, which was formed in this way, with PVA solution, and because the study that the higher the concentration of PVA solution is, the stronger binding effect happens was already proved, the density of PVA was fixed as 2wt% to avoid polymer bridging effect.

The PVA-CNT film was manufactured with PVA-CNT composite solution which was produced through those processes by using drop casting method and adjusting mass ratio of PVA and CNT as 1:10, 1:8, 1:5, 1:2, 1:1, 2:1, 5:1, 8:1, 10:1 each. In this process, it was confirmed that dispersion of CNT doesn't exist effectively in polymer matrix from the point over 1:1 of mass ratio of PVA and CNT, and looks like isolated island through SEM image, and it was analyzed that this morphology has relationship with conductivity.

The conductivity of PVA-CNT composite film showed conductivity of  $4.2 \cdot 10^{-6} \text{S/cm}$  at the film PVA-CNT mass ratio 10:1, but it was increased sharply passing the point PVA-CNT mass ratio 8:1, it reached to around  $1.9 \text{S/cm}$  conductivity when CNT became 10 times of PVA mass.

## References

- [1] Guo-dong Zhan et al., Appl. Phys. Lett., 2003, **Vol. 83**, No.6
- [2] Pedro Henrique Cury Camargo et al., Materials Research, 2009, **Vol. 12**, No. 1, 1–39
- [3] Q. Cao et al., Nature, 2008, **454**, 495–500.
- [4] Seung Woo Lee, Naoaki Yabuuchi et al., Nature Nanotechnology, 2010, **5**, 531–537
- [5] Chen Q, Saltiel C, Manickavasagam S, et al. J colloid Interf Sci, 2004, 280: 91–97
- [6] Marc Chaouat et al., Adv. Funct. Mater., 2008, 18, 2855–2861
- [7] Yaodong Liu, Satish Kumar et al., ACS Appl. Mater. Interfaces, 2014, 6, 6069–6087
- [8] Yaodong Liu, Satish Kumar et al., Polymer Reviews, 2012, 52: 234–258
- [9] B dingm M Wang et al., Sensors, **2009**, 9, 1609–1624
- [10] Michael F. L. De Volder, A. John Hart et al., Science, **2013**, Vol. 339 no.6119, 535–539
- [11] Mauro Ferrari., Nature Reviews Cancer, 2005, **5**, 161–171
- [12] D.R. Paul, L.M. Robeson., Polymer, 2008, **49**, 3187–3204
- [13] M. Calvaresi, M. Quintana, et al., Chemphyschem, **2013**, 14, 3447–3453
- [14] F. Yang et al., Nature, 2014, **510**, 522–524
- [15] Carbon Nanotube Reinforced Composites: Metal and Ceramic Matrices. S. C. Tjong Copyright, **2009**, WILEY-VCH Verlag CMbH&Co. KGaA, Weinheim, ISBN:978-3-527-40897-4
- [16] S. Iijima, Nature, 1991, **354**, 56–58
- [17] S. Iijima, T. Ichihashi., Nature, 1993, **363**, 603–605
- [18] P.-C. Ma et al., Composites: part A, 2010, 41, 1345–1367
- [19] H. Lee et al., Adv. Energy Mater., 2012, 2(8), 976–982
- [20] N. Malachi et al., Angewandte., 2012, 124(7), 1600–1603
- [21] N. Hu et al., Acta Materialia., 2008, **56**, 2929–2936
- [22] A. M.K. Esawi et al., Materials and Design., 2007, 28, 2394–2401
- [23] W. Lyoo et al., Intern. J. Polymeric Mater., 2000, 46, 181–194
- [24] K. Choi et al., Polymer Sci Technol(Korea)., 2004, 15(1), 4–11

- [25] J. P. Kim et al., *Polymer Sci Technol(Korea)*, 2004, 15(1), 31–37
- [26] J. W. Essam., *Rep. Prog. Phys.*, 1980, 43, 835–909
- [27] K.K. Mohanty et al., *Chemical Engineering Science*, 1982, 37(6), 905–924
- [28] D. K. Schroder., *Semiconductor material and device characterization*. John Wiley & Sons., 2006.
- [29] J. D. Weiss et al., *Solid-State Electronics*, 2008, 52, 91–98
- [30] R.S. Dacosta et al., *J. Gastroenterol. Hepatol.*, 2002, 17(suppl), S85-S104
- [31] H. Suda et al., *Adv. Dent Res.*, 1997, 11, 539-547.
- [32] A. Montazeri et al., *Advanced materials research*, 2011, 264, 1954–1959
- [33] K. A. Wepasnick et al., *Anal Bioanal Chem.*, 2010, 396, 1003–1014
- [34] M. S. Dresselhaus et al., *Nano letters*, 2010, 10(3), 751–758
- [35] A.J. Blanch et al., *J. phys. Chem. B.*, 2010, 114, 9805
- [36] S. Dolle et al., *Angewandte*, 2012, 51(13), 3254–3257
- [37] O. Spalla and B. Cabane., *Colloid Polym Sci*, 1993, 271, 357–371
- [38] Y. Otsubo and M. Horigome., *Korea-Australia Rheology Journal*, 2003, 15(1), 27–33

## 요약 (국문초록)

Carbon NanoTubes (CNTs) 물질은 뛰어난 전기적 특성으로 인해 산업의 응용에 있어 오랫동안 관심을 받아 왔지만, 이러한 탄소물질은 다른 고분자물질과 복합체 형성에 있어 분산문제가 항상 대두되어 왔으며, 특히 이러한 CNT 물질이 산업 응용에 있어 가장 큰 장애물인 응집체를 만드는 현상은 CNT 간에 작용하는 Van Der Waals 힘에 의하여 일어난다.

CNT 간의 Van Der Waals 힘에 의한 인력은 CNT가 계 내에서 CNT의 탄소원자가 다른 CNT 분자의 탄소고리 중심과 가깝게 인접할수록 형성된다. 이러한 현상 때문에, CNT 입자는 큰 응집체를 매우 쉽게 형성한다. 따라서, 용매 내에서 CNT를 완전히 분산하기란 쉽지 않으며, 분산이 잘 되지 않을 경우 Percolation model을 형성하는데 필요한 CNT의 양이 증가하게 된다. 이는, 필름 내에서 전도특성을 가지는 통로를 형성함에 있어 CNT 물질이 지나치게 많이 소모될 수 있음을 의미한다.

특히 CNT가 고분자와 복합체를 형성할 경우에도, 전도특성 측면에 있어 응집된 CNT는 결함을 불러온다. 그러므로 본 연구에서는 안정적으로 잘 분산된 CNT 분산용액을 계면활성제의 도입을 통하여 제작하였고, 이를 통하여 PVA 고분자와 복합체 필름을 제작하였다.

먼저, 최적의 조건에 분산된 CNT 용액을 만들기 위하여 계면활성제로써 양이온성의 계면활성제인 Hexadecyl trimethyl ammonium bromide (CTAB) 물질을 이용하였고 Tip-sonication을 통하여 CNT 분산용액을 제작하였다. 이 과정을 통하여 CNT에

손상을 주지 않는 동시에 분산에 알맞은 최적의 sonication 시간이 존재함을 확인하였다. 더욱이, 분산을 위한 sonication 시간이 길어질 경우 CNT 에 손상이 가해지는 것을 Raman spectroscopy 를 통해 분석하였다.

이러한 이유로 우리는 최대한 CNT 에 가해지는 손상을 피하면서 매우 잘 분산된 CNT 용액을 얻기 위하여 최적의 분산시간 이후에 잔여 응집체를 원심분리를 통하여 제거 한 뒤 Lambert-Beer 법칙에 따라 손실률을 계산하고 최종적으로 얻어진 상청액을 PVA 고분자 용액과 복합하였다.

분산에 영향을 미치는 모든 조건을 최적화 한 후 만들어진 PVA-CNT 복합체 용액을 통하여 전도도를 갖는 PVA-CNT 복합필름을 drop-casting 법으로 제작 한 뒤 전도측정을 수행하였다. PVA-CNT의 질량비가 10:1인 필름에서  $4 \cdot 10^{-6}$  S/cm 정도의 전도성을 나타냄을 확인하였고 질량비가 8:1이 되는 지점부터 전도도가 급격히 상승하기 시작하여 PVA-CNT 의 질량비가 1:10이 되는 지점에서 전도도가 2 S/cm 정도 까지 도달함을 분석하였다.

**주요어(5) :** 탄소나노튜브, 고분자 복합체, 폴리비닐알콜, 필름, 전도도

**학번 :** 2012-22450